Probing the particle acceleration at trans-relativistic shocks with GRB afterglows

Kazuya Takahashi (YITP, Kyoto U.)
Kunihito Ioka (YITP, Kyoto U.)
Yutaka Ohira (U. Tokyo)
Hendrik van Eerten (U. Bath)

Neutron Star Merger GW170817

EM counterparts

short GRB
GRB 170817A

kilonova（optical, IR）

GRB afterglow（radio, optical, X-ray）

Multi-Messenger Astronomy!

picture: from LIGO website

Afterglow of GRB170817A

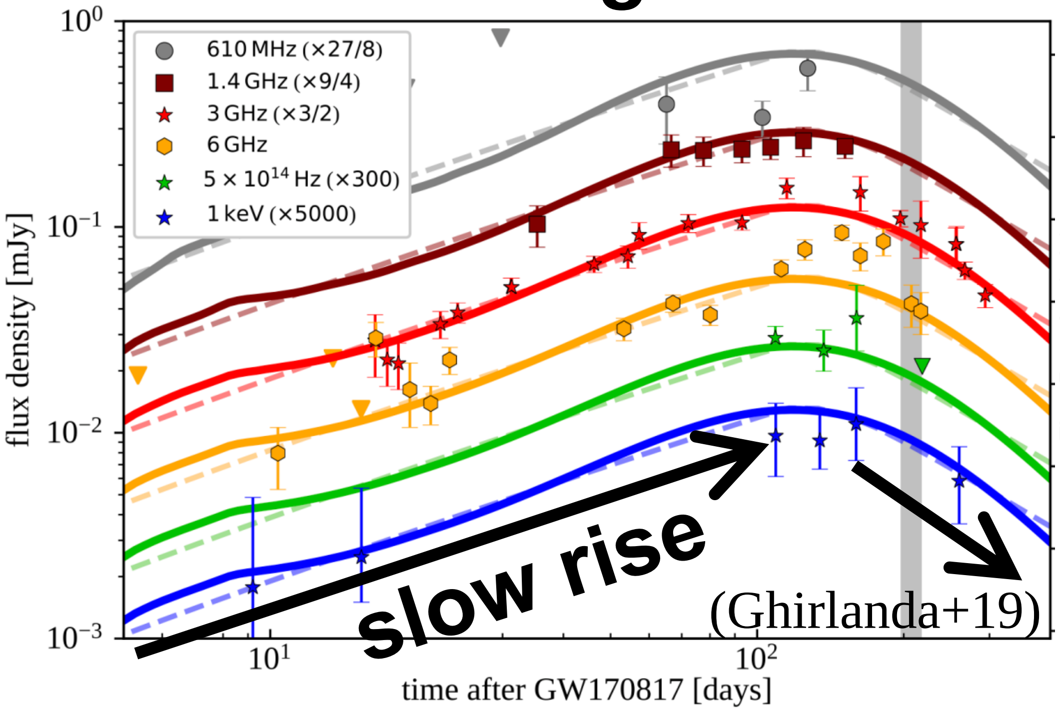

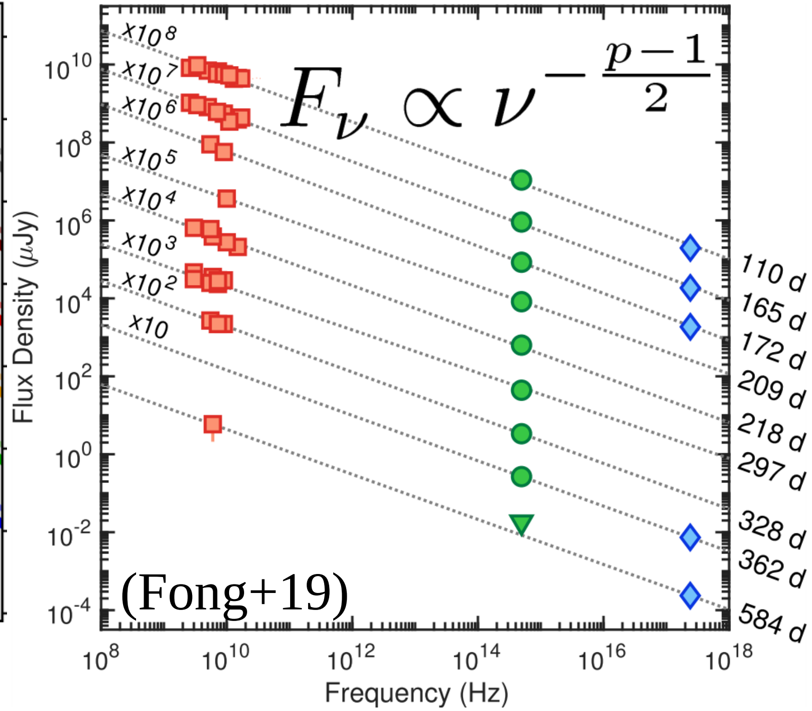

- slow rising & rapid decline after the peak
- single power-law spectrum
- super-luminal motion of a compact source detected by VLBI

＊Synchrotron radiation from a relativistic jet

＊The jet is structured and is viewed from off-axis.

Spectrum: a single power-law from radio to X-ray

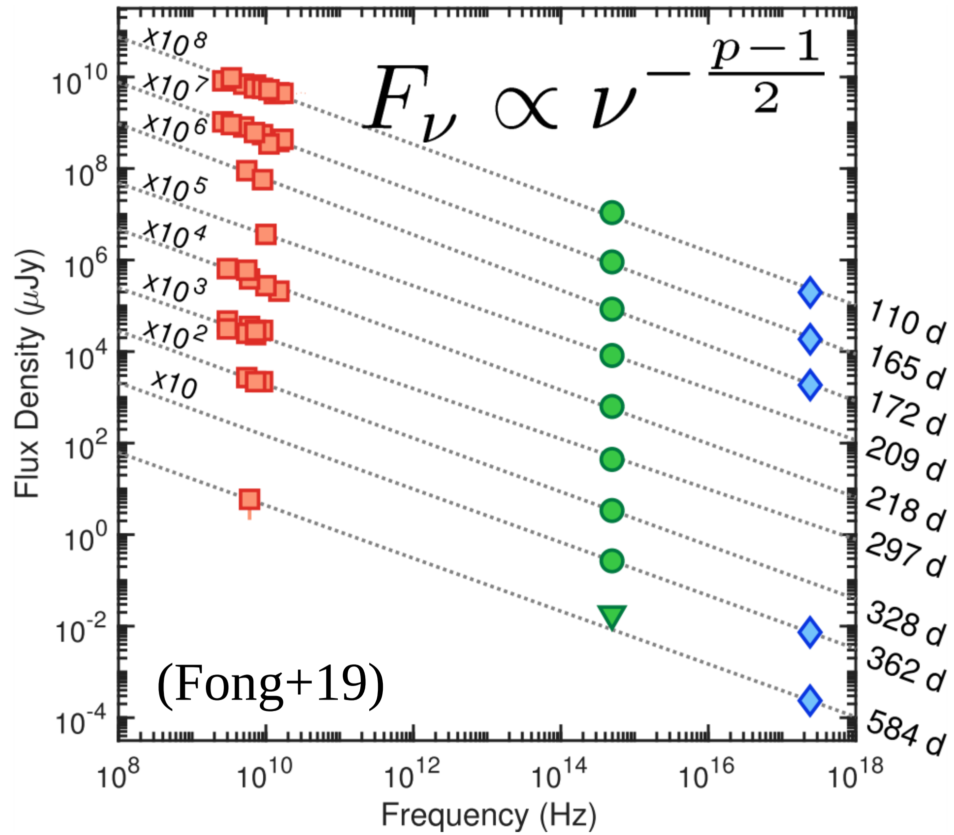

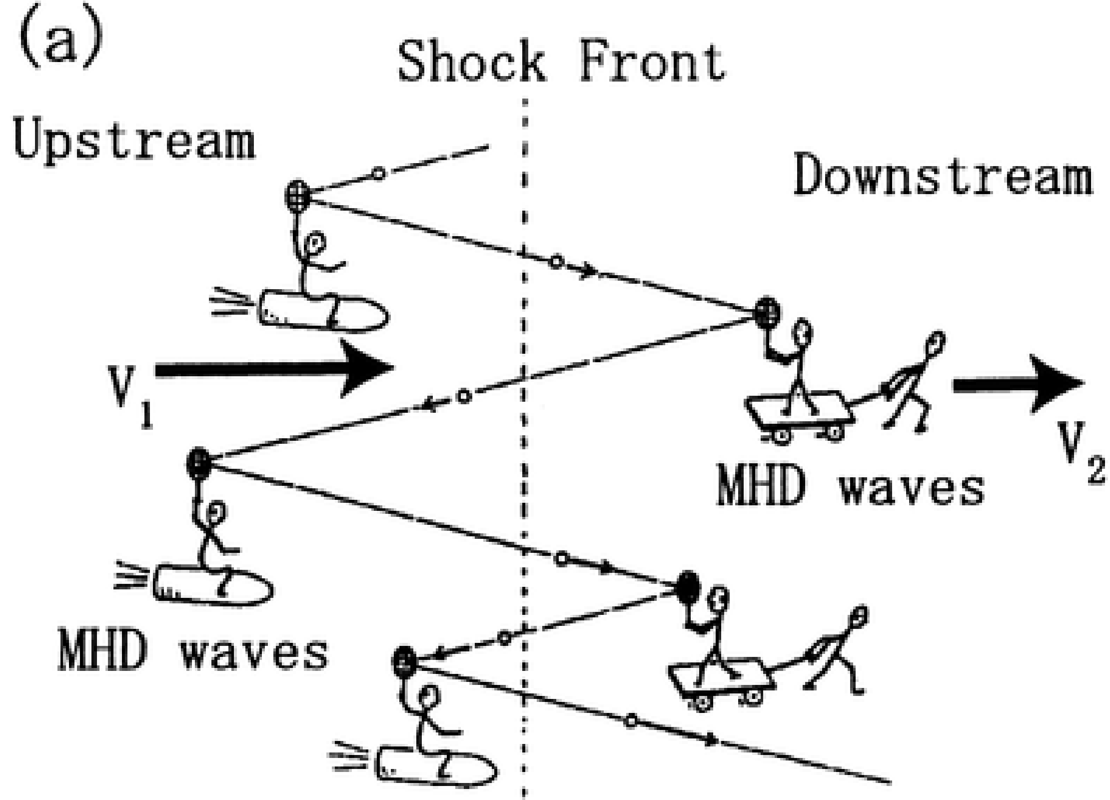

p: energy spectral index of the accelerated electrons

$$f(E)\mathrm{d}E \propto E^{-p}\mathrm{d}E$$

Spectrum: a single power-law from radio to X-ray

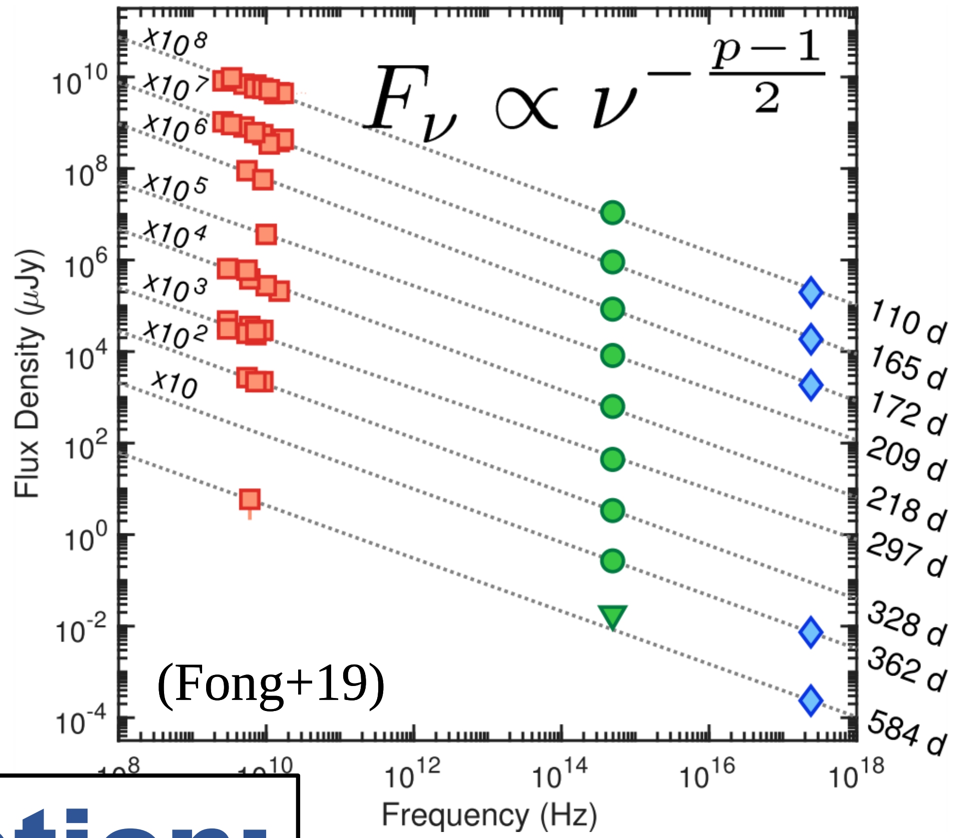

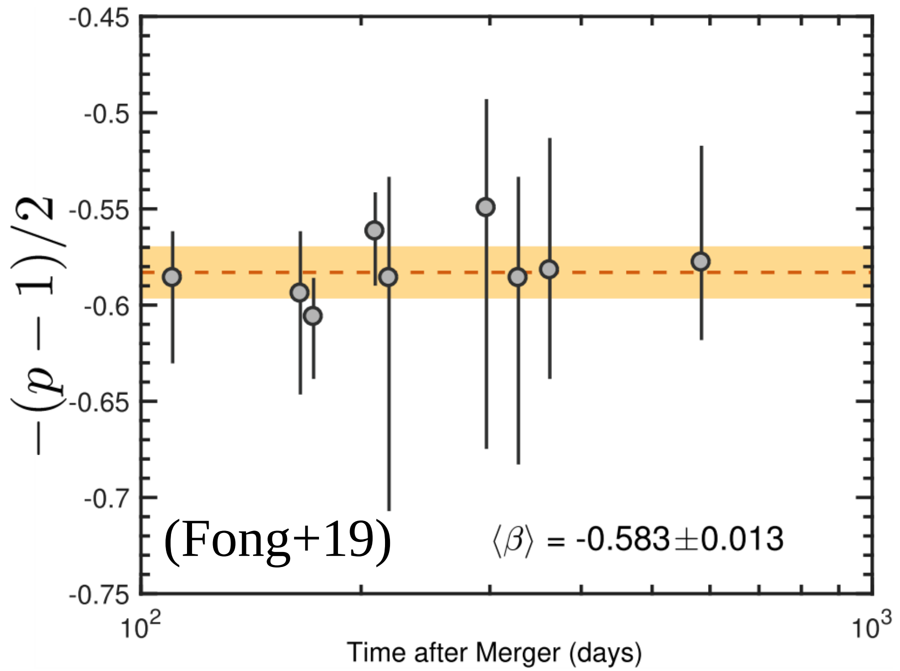

It is consistent with *p* = const.
But, the obs. errors are large.

Question:

Can we obtain the evolution of *p* more precisely in future observations of off-axis GRB afterglows?

Motivation:

1. Short GRBs can take place in a dense environment. Afterglow fluxes become larger for denser ISM.

ISM number density in short GRBs

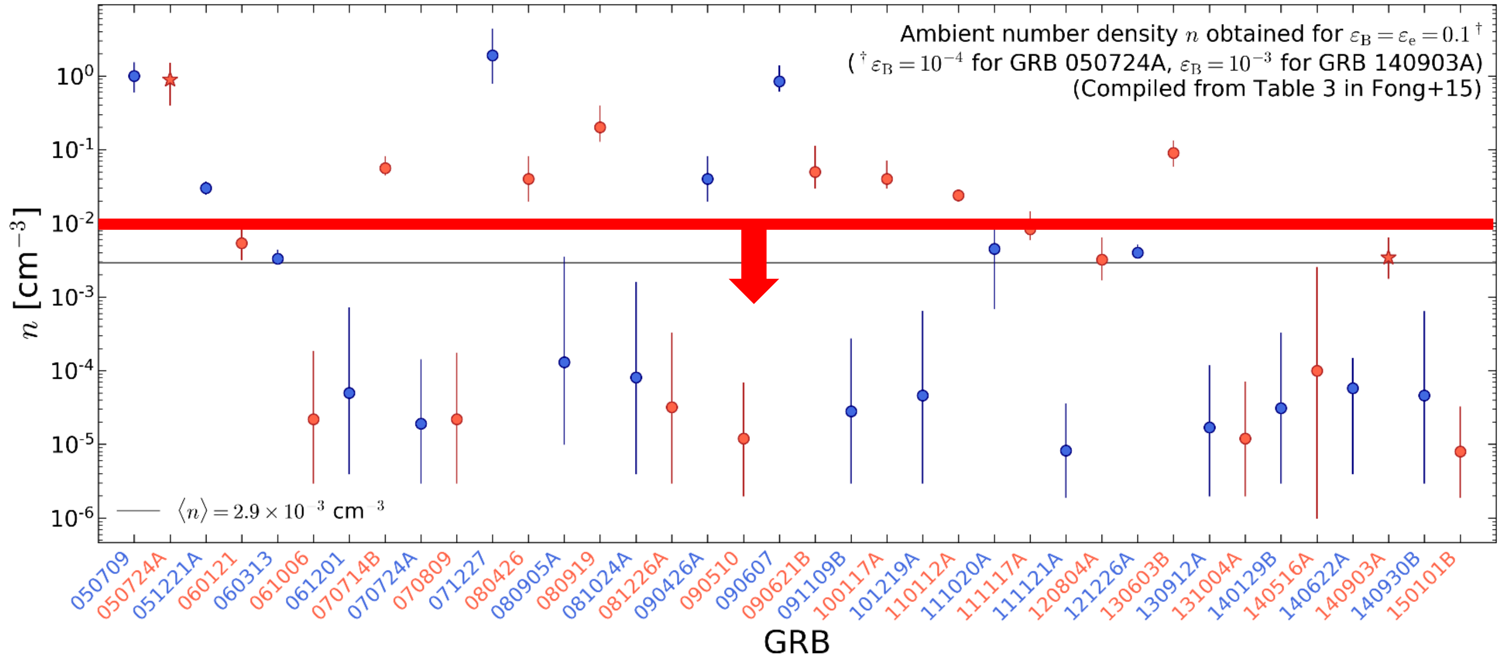

upper limit for GRB 170817A (Hajela+19)

2. Afterglows of nearby (D< 200 Mpc) off-axis short GRBs will be detected as a counterpart of gravitational wave signals.

Method

Off-axis afterglow model:

Electrons are accelerated at the forward shock.
We assume an acceleration model $p = p(\Gamma_{\rm sh})$

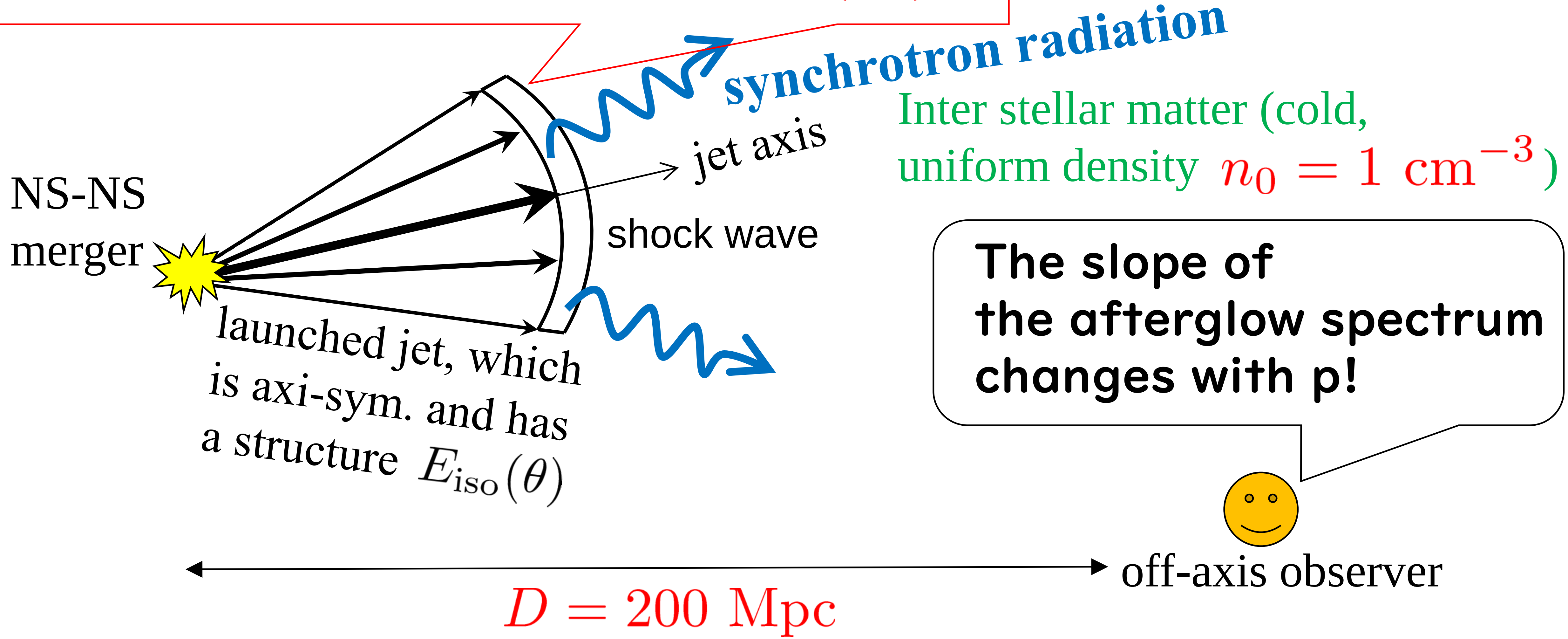

Observed afterglow flux (Sari+98, Granot+99, van Eerten+10)

$$F_\nu(T) = \frac{1}{4\pi D^2}\int d\Omega\, \mu R^2 \left.\frac{\epsilon'_{\nu'}(1-e^{-\tau_\nu})}{\alpha'_{\nu'}\Gamma^3(1-\beta\mu)^3}\right|_{t=t(T,\Omega)}$$

Local synchrotron emission

$\epsilon'_{\nu'}(E_{\rm iso}, n_0, \varepsilon_B, \varepsilon_e, p)$: emissivity

$\alpha'_{\nu'}(E_{\rm iso}, n_0, \varepsilon_B, \varepsilon_e, p)$: absorption coefficient

$p=p(\Gamma_{sh})$: electron power-law index

n_o : ISM number density

$\varepsilon_{\rm B}$: energy conversion fraction to B-field

$\varepsilon_{\rm e}$: energy conversion fraction to e-accel.

τ_ν : optical depth

μ : cosine of the angle btw. the radial direction and the line of sight

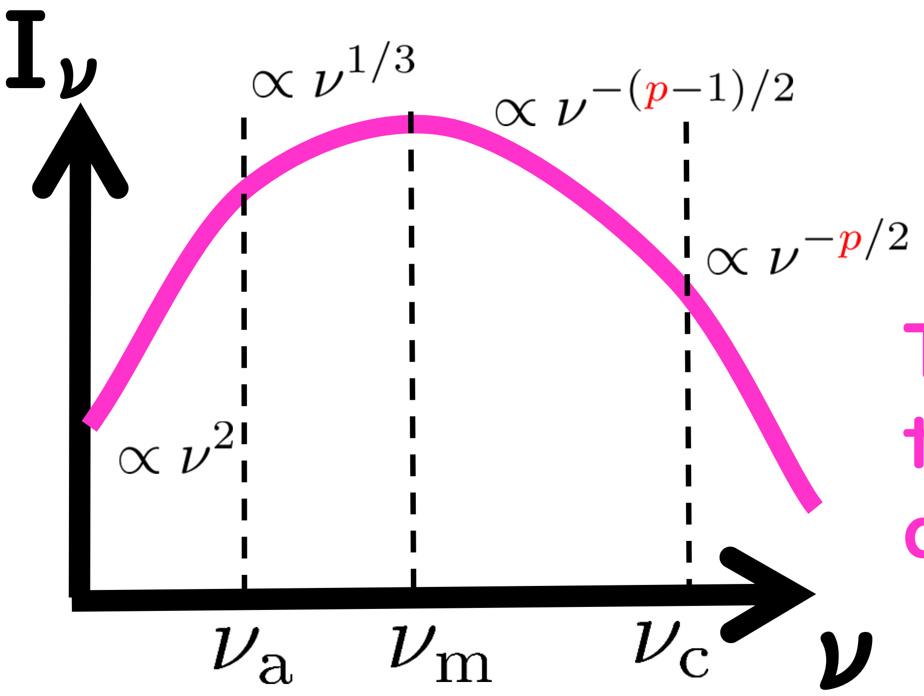

The shape of the spectrum depends on *p*

Shock dynamics model

- Each segment expands as if it were a portion of a spherically expanding shell.
- Blandford & McKee 1976 (Rela. regime) + Sedov & Taylor (Non-rela regime)
- Thin shell approximation

Particle acceleration model

As an example, we use the model of **Keshet & Waxman (2005)**:

* parallel shock
* isotropic diffusion
* Relativistic effects

$$p = \frac{3\beta_u - 2\beta_u\beta_d^2 + \beta_d^3}{\beta_u - \beta_d} - 2$$

$\beta_{u,d}$: shock upstream& downstream speeds measured at the shock rest frame

Relativistic limit:

$$p \to 2.22 \ (\Gamma_{\rm sh} \to \infty)$$

Non-relativistic limit:

$$p \to 2 \ (\Gamma_{\rm sh} \to 1)$$

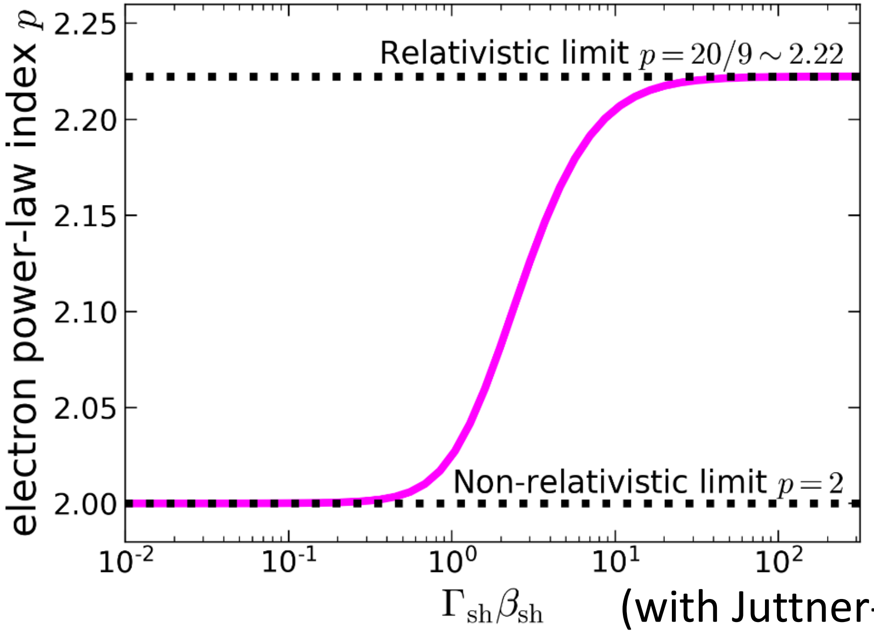

(with Juttner-Synge EoS)

* This model is consistent with the afterglow spectra of GRB 170817A. (KT et al., in prep.)

Jet structures and afterglow parameters

We apply three jet structures that are consistent with the afterglow of GRB 170817A for $n_0 = 10^{-3}\ \mathrm{cm}^{-3}$. (KT & Ioka 2021)

The values of afterglow parameters $\varepsilon_{\mathrm{B}}, \varepsilon_{\mathrm{e}}$ are the same as those used for GRB 170817A.

The viewing angle is changed in the range of $0.25 \leq \theta_{\mathrm{v}} \leq 0.5$

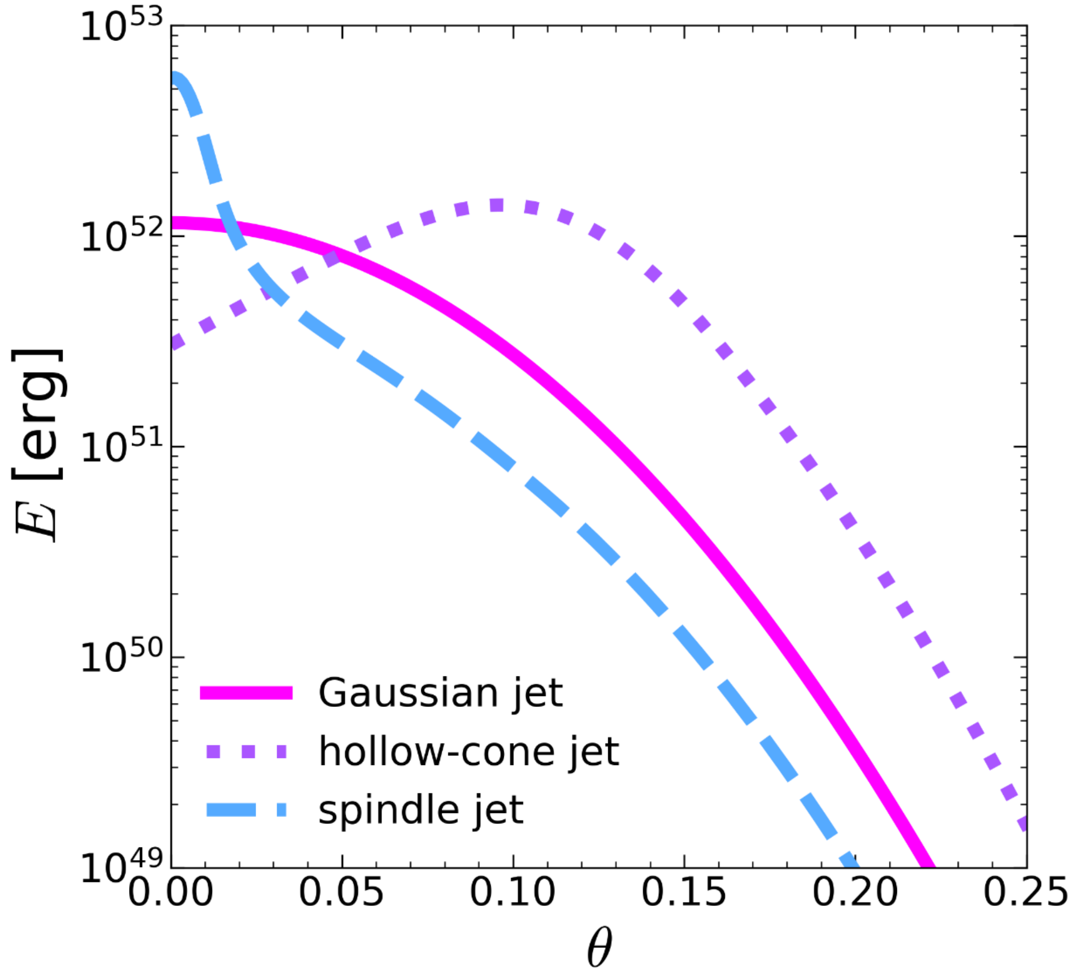

Electron power-law index p derived from the spectral slope

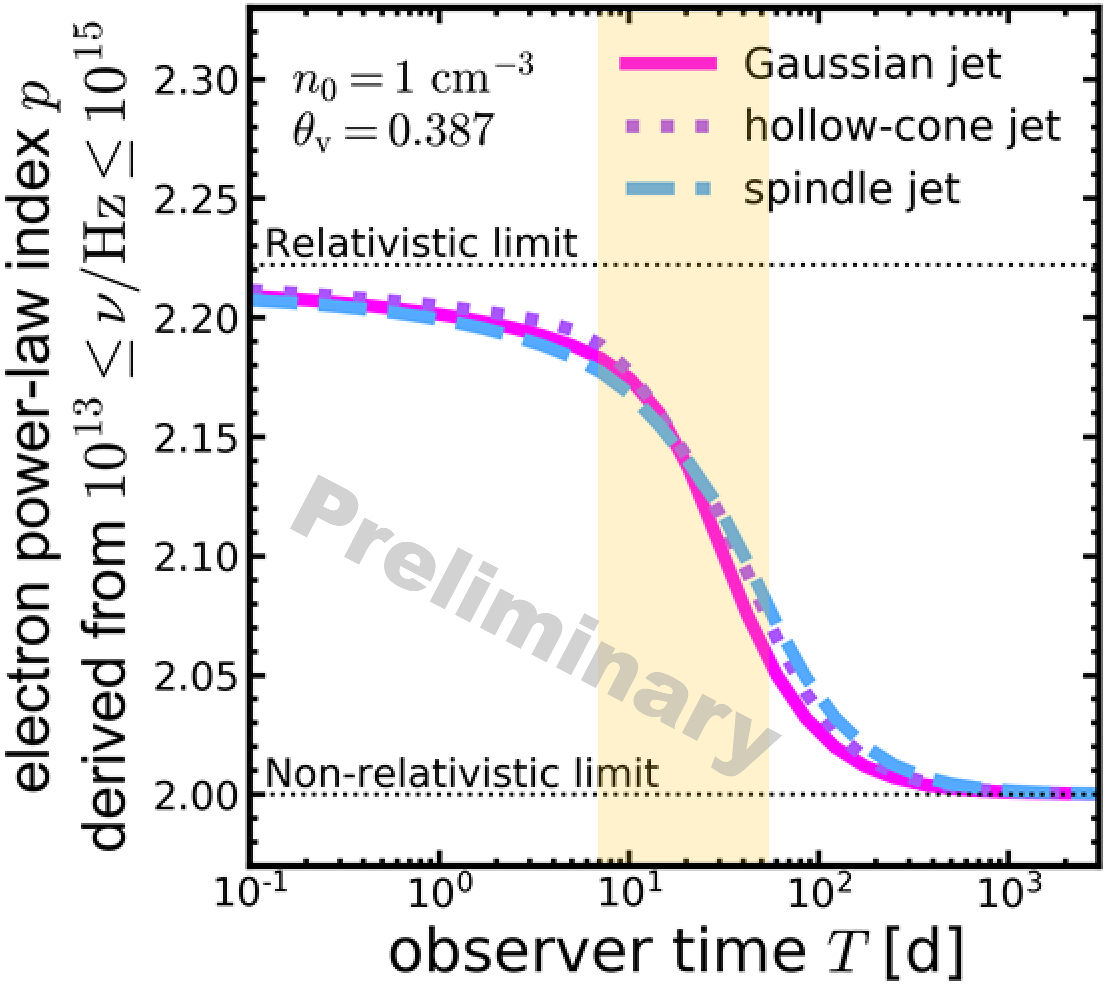

Afterglow light curves

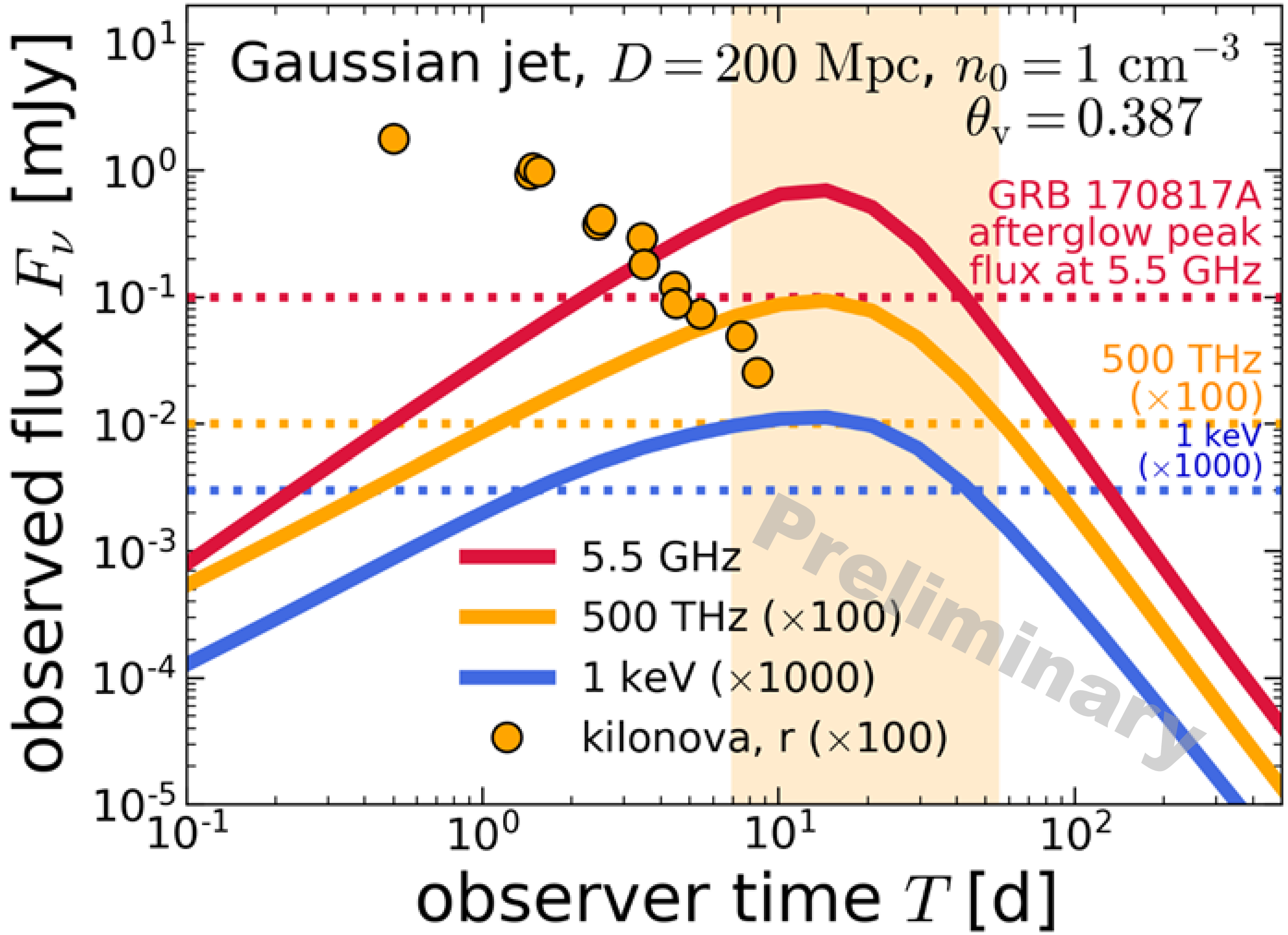

The transition phase of *p* could be observed!

Summary & Conclusion

Off-axis GRBs similar to GRB 170817A, but with

- larger ISM density: $n_0 = 1\ \mathrm{cm}^{-3}$
- larger luminosity distance: $D = 200\ \mathrm{Mpc}$
- similar viewing angle: $0.25 \leq \theta_{\mathrm{v}} \leq 0.5$

➡ The transition of the electron power-law index p from relativistic to non-relativistic regimes would be observable in more luminous afterglow than for GRB 170817A.

Backup

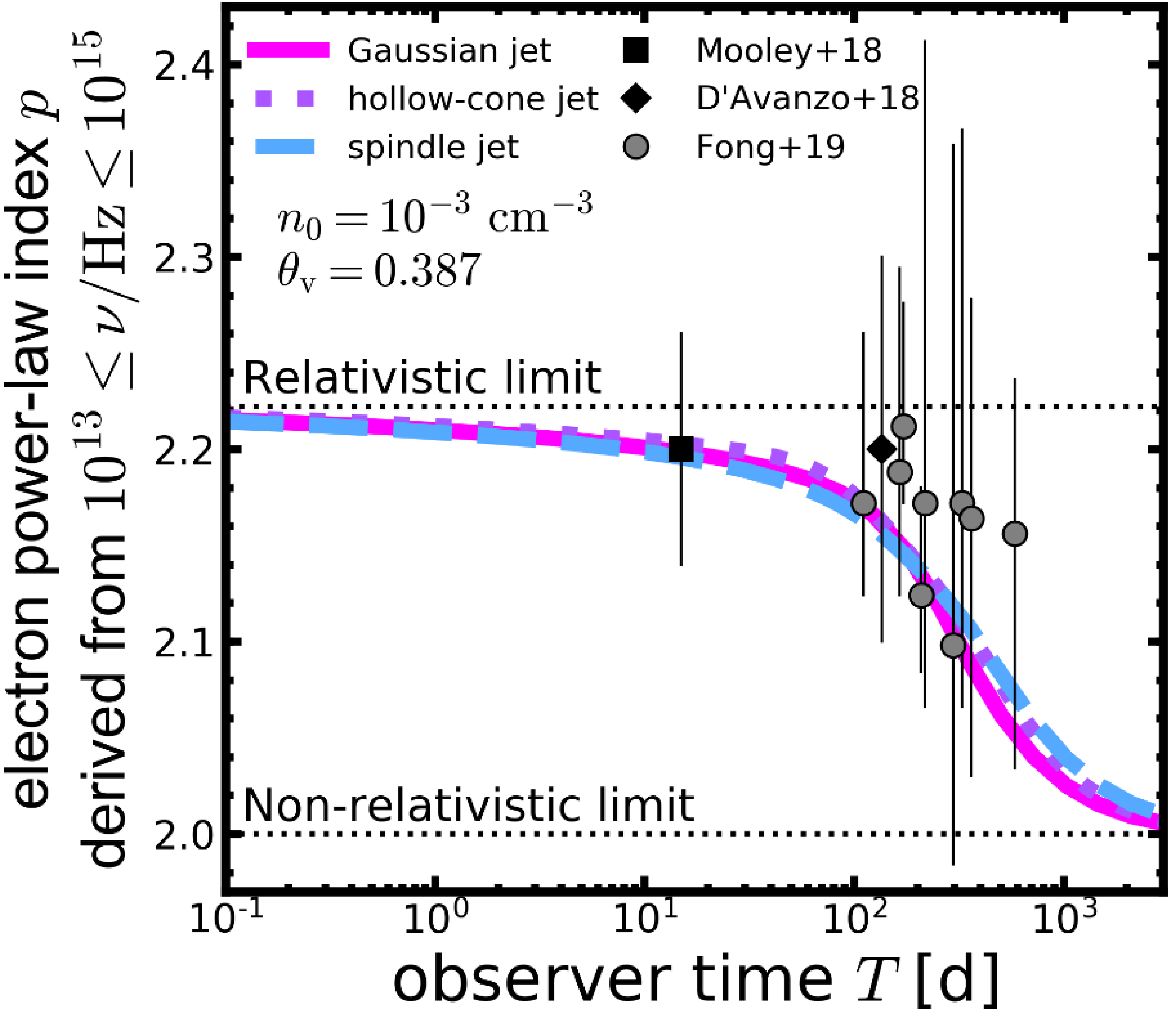

Gaussian jet
hollow-cone jet
spindle jet
Mooley+18
D'Avanzo+18
Fong+19
$n_0 = 10^{-3}$ cm^{-3}
$\theta_{\rm v} = 0.387$
Relativistic limit
Non-relativistic limit
electron power-law index p
derived from $10^{13} \leq \nu/\mathrm{Hz} \leq 10^{15}$
observer time T [d]
2.0
2.1
2.2
2.3
2.4
10^{-1}
10^{0}
10^{1}
10^{2}
10^{3}

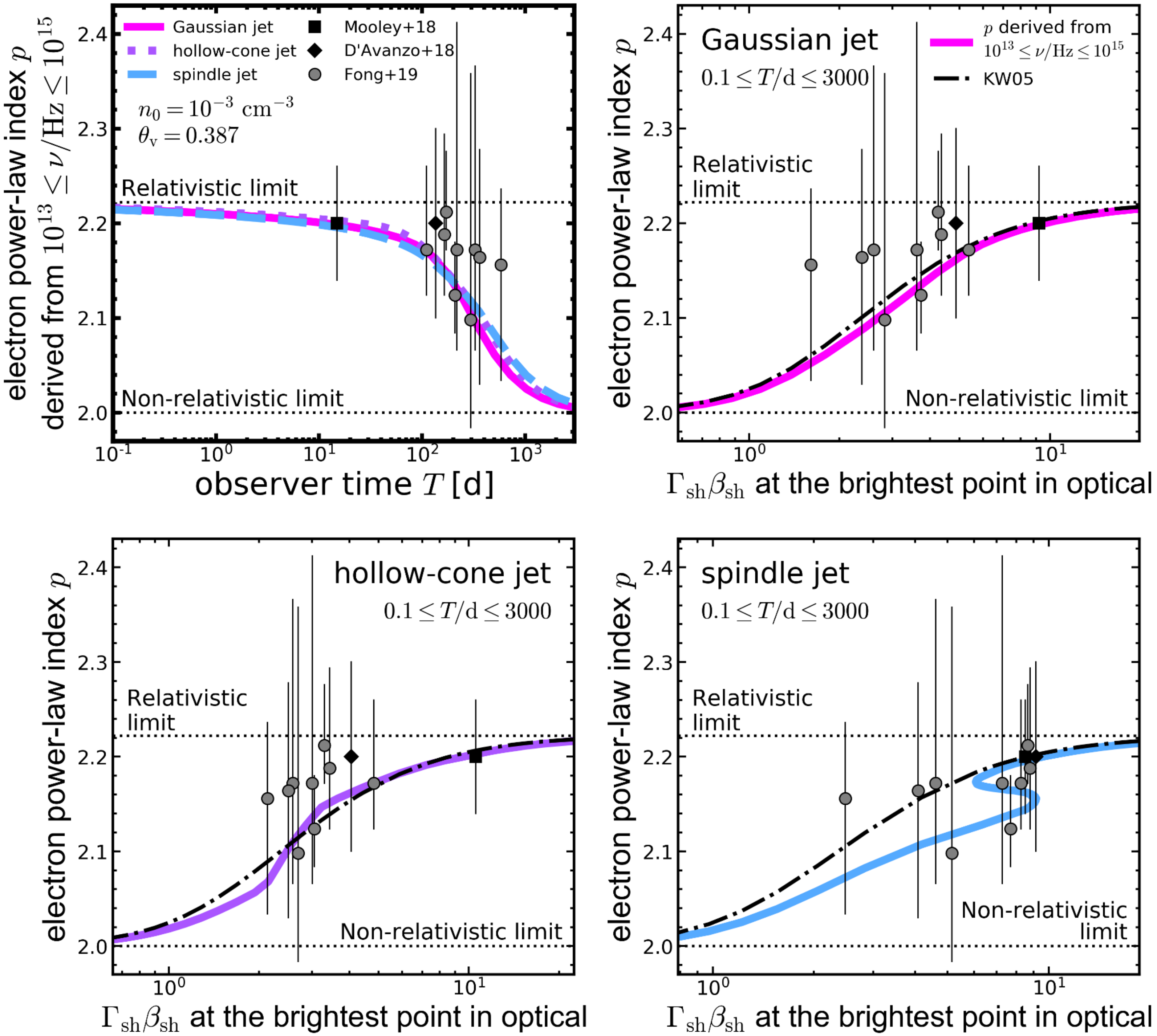

Gaussian jet
hollow-cone jet
spindle jet
Mooley+18
D'Avanzo+18
Fong+19
$n_0 = 10^{-3}$ cm^{-3}
$\theta_v = 0.387$
Relativistic limit
Non-relativistic limit
electron power-law index p derived from $10^{13} \le \nu/\mathrm{Hz} \le 10^{15}$
observer time T [d]
Gaussian jet
$0.1 \le T/\mathrm{d} \le 3000$
p derived from $10^{13} \le \nu/\mathrm{Hz} \le 10^{15}$
KW05
electron power-law index p
$\Gamma_{\mathrm{sh}}\beta_{\mathrm{sh}}$ at the brightest point in optical
hollow-cone jet
$0.1 \le T/\mathrm{d} \le 3000$
spindle jet
$0.1 \le T/\mathrm{d} \le 3000$

Smaller viewing angle

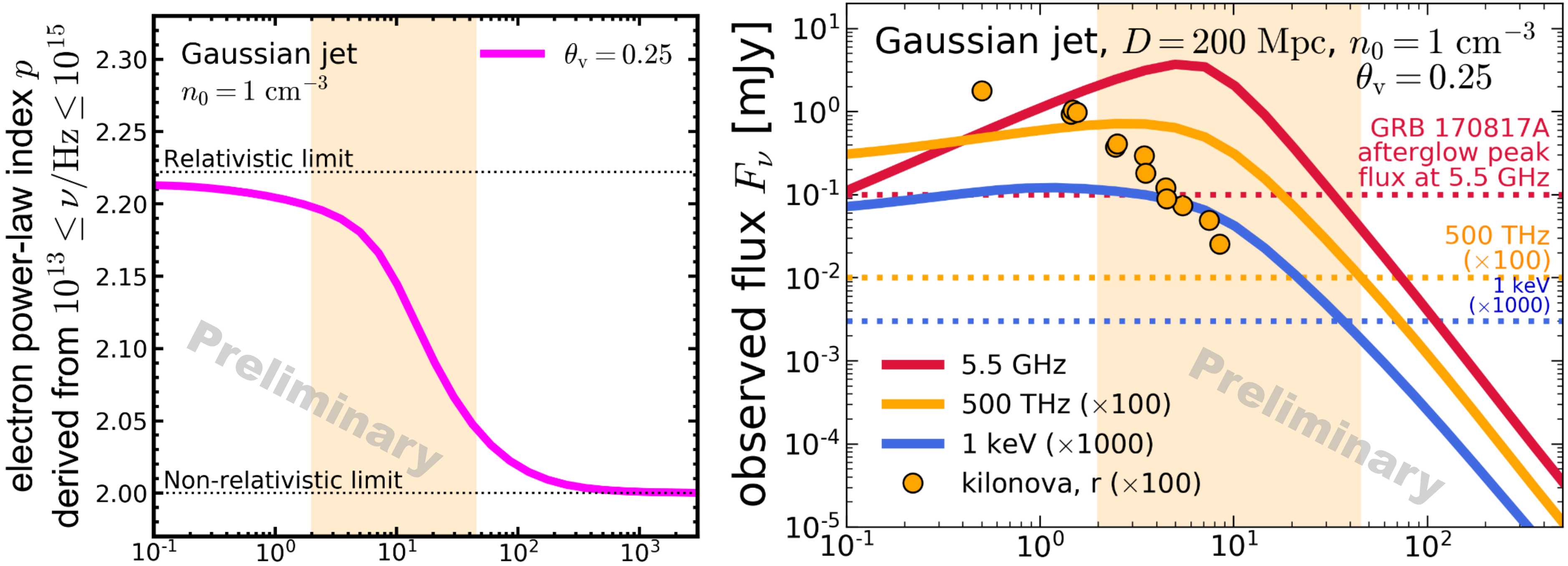

Larger viewing angle

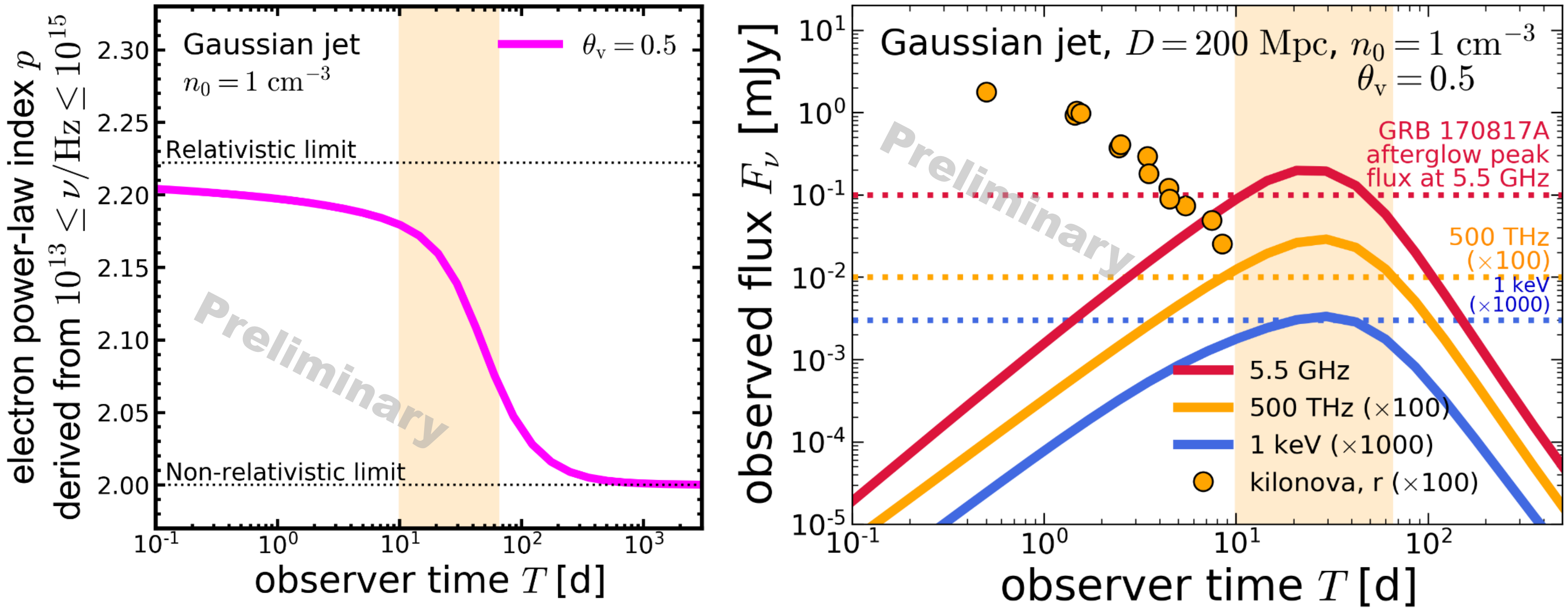

Structured jet + off-axis

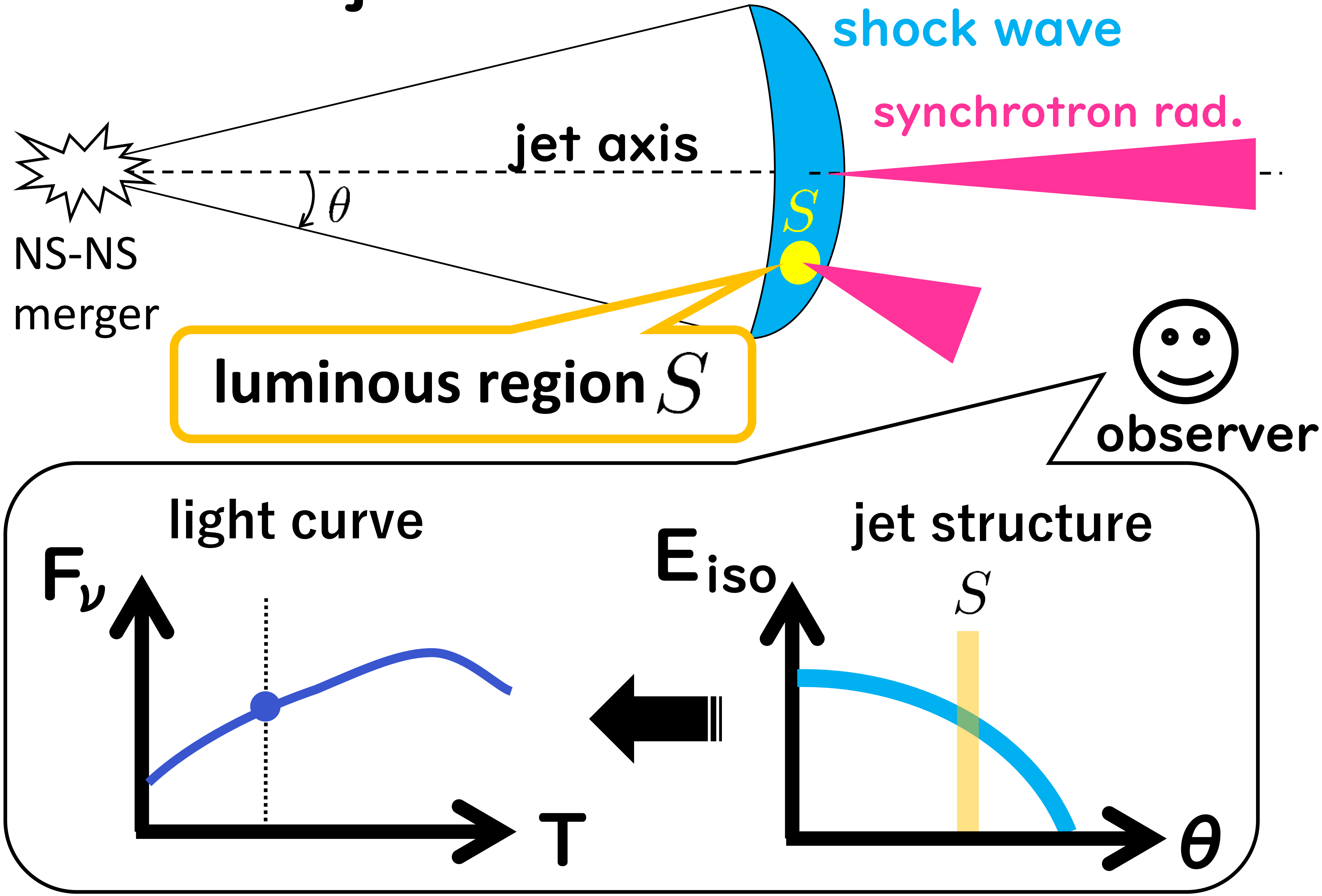

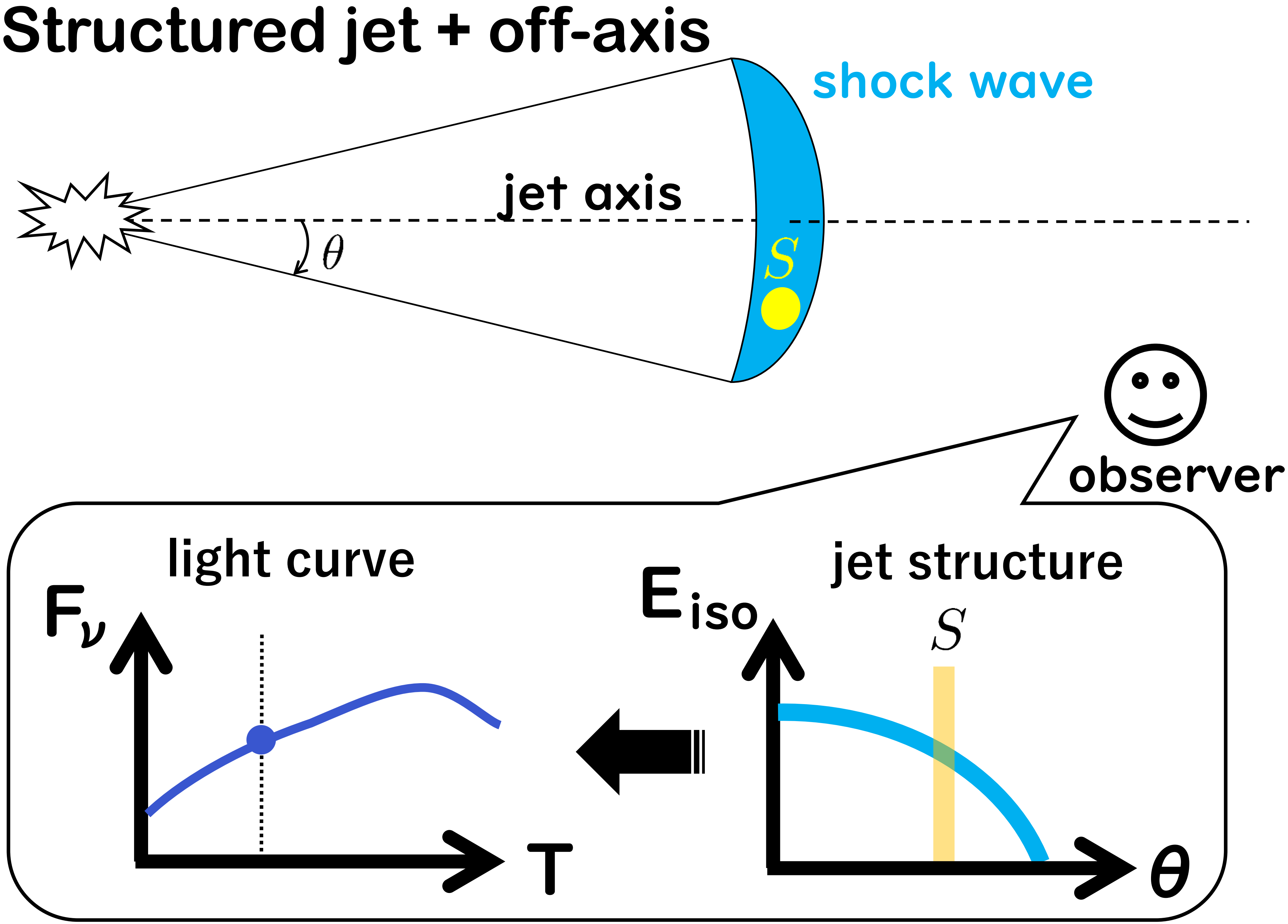
Structured jet + off-axis
shock wave
jet axis
θ
S
observer
light curve
F_ν
T
jet structure
E_iso
S
θ

Diversity of the possible jet structures (KT & Ioka 2020, 2021)

Jet structure

Afterglow light curve

Hollow-cone jet

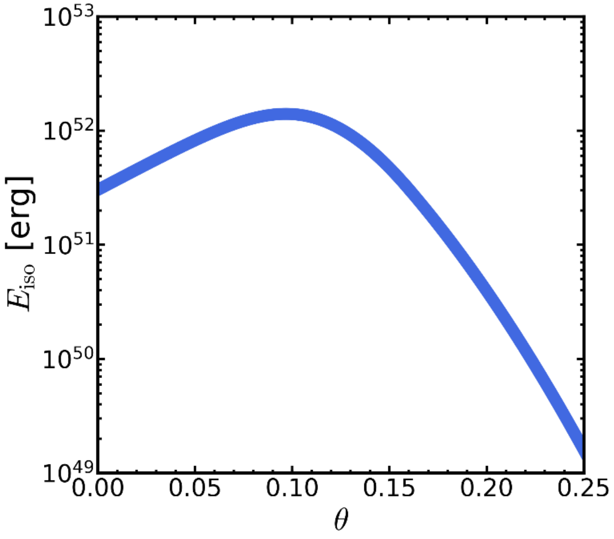

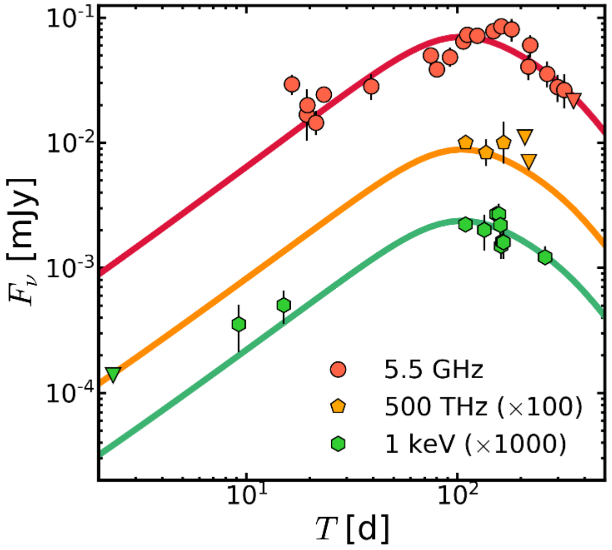

consistent with the observations!

Spindle jet

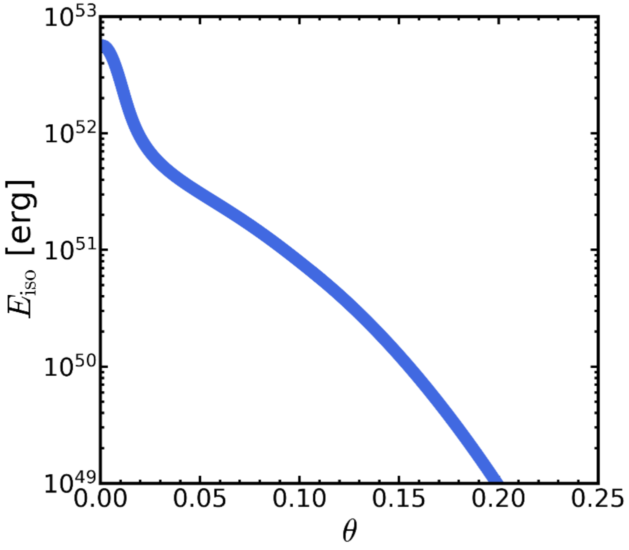

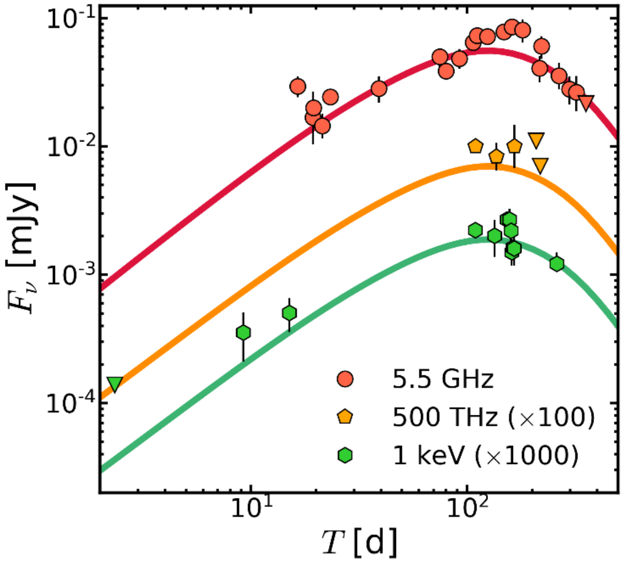

consistent with the observations!

Gaussian jets and power-law jets are also candidates.